HIGH CYCLE MULTIAXIAL FATIGUE

D. L. McDiarmid
City University, London, U.K.

Abstract

A number of different cases of crack growth which can occur under multiaxial fatigue stress situations, dependent on the particular multiaxial loading conditions being applied, are discussed. These different cases of crack growth are discussed in detail in relation to multiaxial fatigue stress test data in the literature for loading conditions such as combined bending and twisting and also thin and thick cylinders subjected to longitudinal load and differential pressure across the wall thickness. The effects of out-of-phase stresses, mean stress, stresses at different frequencies and different types of stress waveform are also discussed.

A general criterion of failure for high cycle multiaxial fatigue

$$\tau_a/t_{A,B} + \sigma_{n.max}/2\sigma_T = 1$$

is presented and shown to give good correlation with a wide variety of multiaxial fatigue test data.

The criterion is based on a critical plane approach where fatigue strength is a function of the shear stress amplitude and the maximum normal stress on the critical plane of maximum shear stress amplitude, taking into account whether Case A cracks, growing along the surface, or Case B cracks growing inwards from the surface occur.

Nomenclature

α	Frequency ratio = frequency of σ_{2a}/frequency of σ_{1a}
λ	Principal stress amplitude ratio = σ_{2a}/σ_{1a}
ϕ	Out-of-phase angle, where σ_2 leads σ_1; related to σ_2 where one cycle of σ_2 is 360°
$\sigma_1, \sigma_2, \sigma_3$	Principal stresses $(\sigma_1 > \sigma_2 > \sigma_3)$
$\sigma_{1a}, \sigma_{2a}, \sigma_{3a}$	Principal stress amplitude
σ_a	Stress amplitude
σ_A	Uniaxial reversed fatigue strength
σ_m	Mean stress
σ_n	Normal stress amplitude on the plane of maximum range of shear stress
σ_{nm}	Mean normal stress on the plane of maximum range of shear stress.
$\sigma_{n.max.}$	Maximum normal stress on the plane of maximum range of shear stress
σ_T	Tensile strength
$\sigma_{n12}, \sigma_{n23}$ σ_{n31}	Normal stress amplitudes on the 12, 23, 31 planes of maximum range of shear stress
τ	Shear stress amplitude
$\tau_{12}, \tau_{23}, \tau_{31}$	Shear stress amplitudes on the 12, 23, 31 planes of maximum range of shear stress
τ_a	Shear stress amplitude on the plane of maximum range of shear stress
τ_m	Mean shear stress on the plane of maximum range of shear stress
ϵ	Strain amplitude
$\epsilon_1, \epsilon_2, \epsilon_3$	Principal strain amplitudes
ϵ_A	Strain at uniaxial reversed fatigue strength
b	Fatigue strength in bending
t	Fatigue strength in torsion
t_A	Reverse shear fatigue strength for Case A crack growth
t_B	Reversed shear fatigue strength for Case B crack growth
k	Ratio of the external to the internal diameter of a cylinder
K_f	Fatigue stress concentration factor
K_t	Theoretical stress concentration factor
$C_{1\ldots4}, n$	Constants

Introduction

Although it is recognised that fatigue is the principal cause of a high proportion of mechanical failures and despite over one hundred years of research experience, fatigue mechanisms

are still not fully understood. This is partly due to the fact that many components in service are subject to complex multi-axial fatigue stress conditions which make it very difficult to assess how fatigue damage occurs and how this damage accumulates during the life of the component. Common examples of fatigue under multiaxial stress are axles, crank shafts and propeller shafts subjected to combined bending and twisting which can be out of phase and at different frequencies. Pressure vessels and piping are other examples and many notches and geometric discontinuities are subject to such complex stress situations.

Many attempts have been made to derive theories which can cope with this wide range of complex multiaxial fatigue stress situations, usually based on simple laboratory test data such as the uniaxial reversed stress fatigue test. a large number of theories of multiaxial fatigue failure have been proposed and many are reviewed in the literature.[1-4] These theories can generally be divided into three approaches, extension of the static yield criteria to fatigue, energy considerations and the critical plane approach. The relative merits of these approaches are discussed in Fatemi and Socie.[5]

Recent work by McDiarmid[6-8] has shown that uniaxial fatigue is a unique case of fatigue crack growth and that the type of crack growth occurring in any particular conditions of multiaxial fatigue must be taken into account.

It has been shown by Brown and Miller[1] that there are two possible cases of crack growth under biaxial fatigue conditions. Case A arises for negative values of $\lambda = \sigma_2/\sigma_1$ (actually σ_3/σ_1) where the cracks propagate along the surface. Case B arises for positive values of $\lambda = \sigma_2/\sigma_1$, where the cracks propagate inwards from the surface. Case B is more severe than Case A.

Following Miller and Brown[9] the three possible Stage I and Stage II cracking systems can be illustrated as shown in Figure 1. For thin wall tubes subjected simultaneously to constant amplitude alternating longitudinal load and alternating differential pressure across the wall thickness, the 1, 2, 3 principal stresses are related to the longitudinal (L, 1), hoop/transverse (H, 2) and radial (R, 3) directions. Thus the τ_{12} shear stress system causes Case A Stage I and II cracks growing along the surface. The τ_{23} and τ_{31} shear stress systems cause Stage I cracks growing inwards from the surface and Stage II cracks growing either parallel to the surface or inwards from the surface. The latter cracks are Case B which are the more dangerous.

It has been shown [6-8] that such situations can be correlated using a critical shear plane criterion of failure, taking account of the type of crack growth occurring. The failure plane is the plane of maximum principal stress associated with the shear stress plane subjected to the greatest range of shear stress. The shear stress range to failure is decreased in a linear relationship, again dependent on the type of crack growth occurring, according to the maximum value of normal stress, that is the sum of both the mean and amplitude of normal stress, acting on the plane of greatest range of shear stress.

This critical shear plane failure criterion also gives good correlation with multiaxial fatigue test data, again taking account of the type of crack growth occurring, in the presence of mean stress and when the biaxial stresses are out-of-phase and at different frequencies. In the latter case the shear and normal stresses on the planes of maximum range of shear stress are non-proportional and cumulative damage conditions exist. Test data with different types of stress waveform can also be correlated.

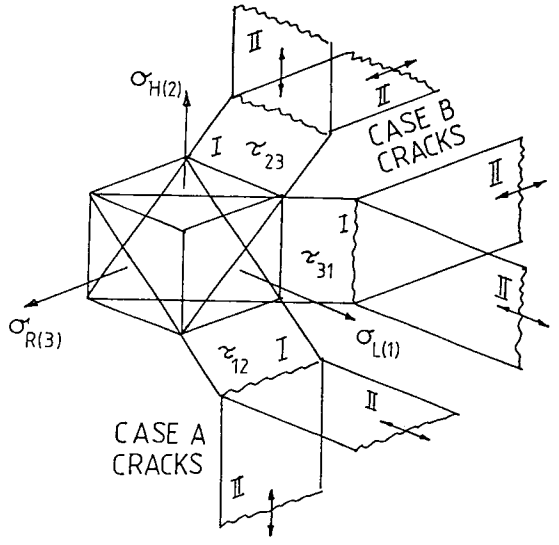

Figure 1.
Crack Growth Planes and Directions From McDiarmid (7).

Theory

The critical shear plane criterion of failure developed in [6] is based on a linear relationship between τ_a and $\sigma_{n,max}$,

$$\tau_a = C_1 - C_2 . \sigma_{n,max.} \qquad (1)$$

When $\sigma_{n.max.} = 0$, that is pure reversed shear fatigue, $C_1 = t_A = t$ for reversed torsion Case A cracking and for Case B cracking $C_1 = t_B$
Extrapolation of the straight line through the test data from [7, 8] shows

that when $\tau_a = 0$ then $\sigma_{n.max} = 2\sigma_T$. The failure criterion can be expressed as

$$\tau_a / t_{A,B} + \sigma_{n.max.} / 2\sigma_T = 1 \qquad (2)$$

in the region $0{\cdot}5t \leq \tau_a \leq t$, $0 \leq \sigma_{n.max} \leq \sigma_T$ as shown in Figure 2.

The reversed shear fatigue strength t_A or t_B is used depending on whether Case A or Case B cracks occur, respectively. In combined bending and twisting Case A cracks occur and $t_A = t$.

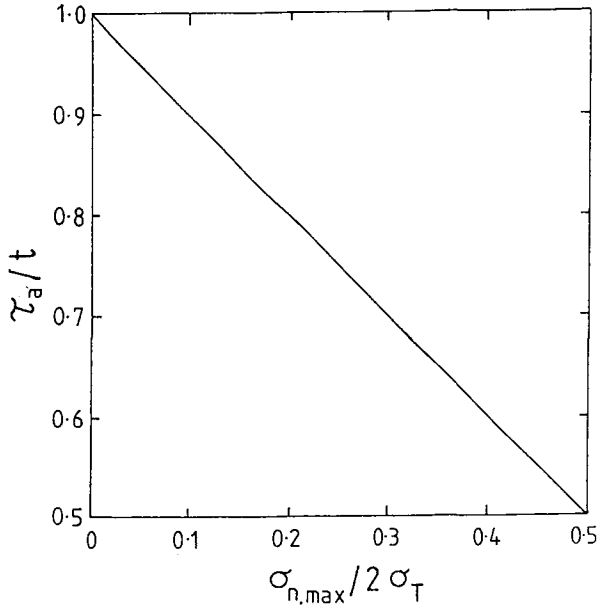

Figure 2.
Criterion of Failure. $\tau_a/t_{A,B}$ Versus $\sigma_{n.max}/2\sigma_T$ In The Working Range.

This new criterion of failure is now applied to the following multiaxial loading conditions, using test data from the literature:-

1. Combined bending and twisting
2. Combined bending and twisting with mean stress
3. Combined bending and twisting, out-of-phase
4. Thin wall cylinders, stresses in-phase
5. Thin wall cylinders, stresses 180° out-of-phase
6. Thin wall cylinders, stresses in phase and out-of-phase at different frequencies
7. Thin wall cylinders with mean stress and out-of-phase stresses at different frequencies
8. Thin wall cylinders with out-of-phase loading including different waveforms and frequencies
9. Thick wall cylinders.

Combined Bending and Torsion

In this type of loading Case A cracks occur and $t_A = t$. Gough et al[10] tested eleven steels, using solid, hollow ad notched specimens under a range of seven ratios of bending to twisting between pure bending and pure twisting. The test data for the solid and hollow test specimens is compared with the failure criterion in Figure 3. The great majority of the data falls within ±5% of the failure criterion. The greatest discrepancies are for materials of high (1.93) and low (1.46) b/t ratios.

Plotting $\tau . K_f/t$ versus $\sigma_{n.max} \cdot K_f/2\sigma_T$ for the notched specimens gives the same results as for the unnotched cases. If K_f is not known and K_t is used then the predicted τ values found will be very small as in these cases K_t/K_f for bending is of the order of 10 and for torsion is of the order of 5 for the lower strength materials and half this for the higher strength materials.

Other[6] combined bending and twisting fatigue test data also gives good agreement with the criterion of failure.

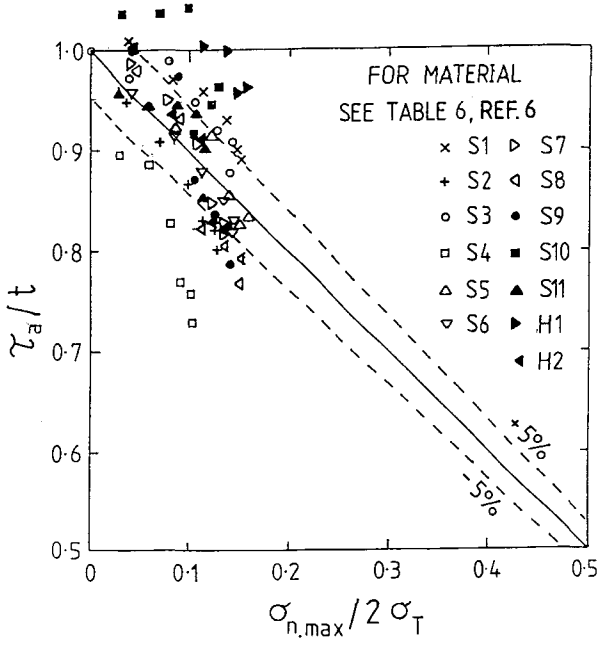

Figure 3.
Correlation of Gough (10) Combined Bending and Twisting Data with Failure Criterion.

Combined Bending and Twisting with Mean Stress

Gough et al[10] also investigated the effect of superimposed bending and torsional mean stresses on the combined stress fatigue limit of a 1000 MN/m^2 tensile strength alloy steel. The data given in Table2 of reference (11) can be used to plot the test data on a τ/t v. $\sigma_{n.max}/2\sigma_T$ basis as shown in Figure 4. Again the data falls within ±5% of the failure criterion.

Combined Bending and Twisting, Out-of-Phase

Nishihara and Kawamoto[12] tested mild steel and hard steel under combined

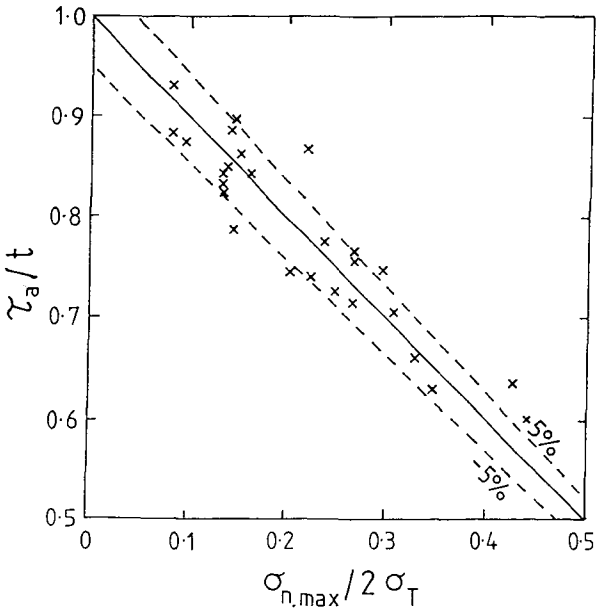

Figure 4.
Correlation of Gough (10) Combined Bending and Twisting with Mean Stress Data with Failure Criterion.

bending and twisting at two stress amplitude ratios and four out-of-phase angles. They showed that the fatigue limits for ductile materials, based on the nominal value of the maximum shear stress, are apparently higher for combined bending and torsion with phase difference than for the conventional in-phase cyclic stressing case. This is so when the out-of-phase fatigue data are presented in terms of the maximum in-phase shear stress amplitudes where the nominal values of the maximum shear stresses in the out-of-phase cases have been calculated using the maximum bending and maximum torsional stress values, neglecting the fact that these stresses do not occur in-phase. Little[13] has shown that this apparent increase in fatigue strength can be misleading, as when the fatigue limit data are expressed in terms of the true maximum shear stress amplitudes in the out-of-phase cases it becomes clear that the fatigue limit actually decreases as the phase difference increases. The decrease is of the order of 25% for a torsion shear stress amplitude to bending stress amplitude ratio of 0.5 and an out-of-phase angle of 90°. This is a special case as all planes in the surface material are planes of maximum range of shear stress.

Further analysis[14] of the Nishihara and Kawamoto[12] data showed that failure was consistent with the plane of maximum range of maximum principal stress and the critical shear planes were taken to be those associated with this principal stress plane. Data in Table 3 of ref. (14) allows the out-of-phase[12] results to be plotted on a τ/t v. $\sigma_{n,max}/2\sigma_T$ basis as shown in Figure 5. The test data falls within ±10% of the failure criterion with the exception of one of the special cases where all planes in the surface material are planes of maximum shear stress as already discussed.

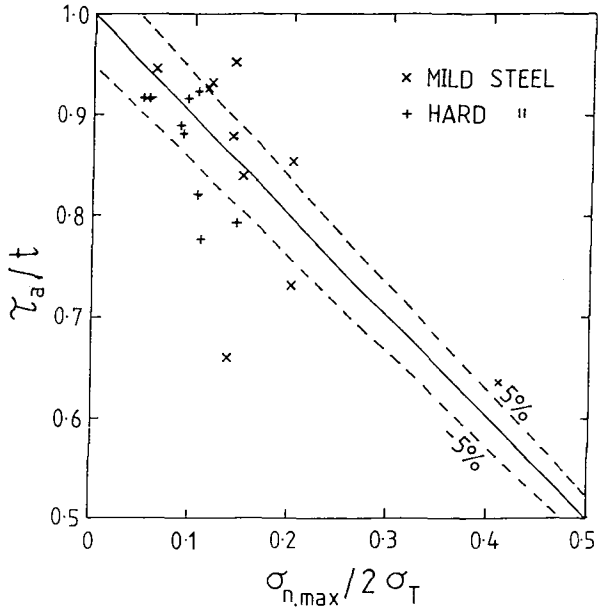

Figure 5.
Correlation of Nishihara and Kawamoto (12) Out-of-Phase Combined Bending and Twisting Data with Failure Criterion.

Thin Wall Cylinders, Stresses In-Phase

McDiarmid[7] tested steel thin wall tubular specimens subjected simultaneously to constant amplitude alternating longitudinal load and alternating differential pressure across the wall thickness under seven values of principal stress amplitude ratio (λ) between 0 (longitudinal stress only) and ∞(transverse stress only) as shown in Table 1 for test cases 1 to 7.

In these tests four different types of crack growth, as illustrated in Figure 6, were identified for λ values as follows: 0 (A/B transverse, circular crack front), 0.25 and 0.5 (B transverse), 0.75, 1,2 (B longitudinal) and ∞ (A longitudinal), as indicated in Table 2, where stresses on the critical shear planes are also shown.

The correlation of all thin wall cylinder test data with the failure criterion is discussed later.

Thin Wall Cylinders, Stresses 180° Out-of-Phase

Tests[7] were also conducted at λ = 0.5, 1, 2 and 3 at an out-of-phase angle of 180°, as shown in Table 1 for cases 8 to 11. All cracks were Case A longitudinal except for λ = 3 where cracks were Case B longitudinal, as indicated in Table 2.

Case	λ σ_{2a}/σ_{1a}	Phase Angle ϕ	Frequ. of σ_2 /Frequ. of σ_1 α
1	0	(longitudinal stress only)	
2	0.25	0	1
3	0.5	0	1
4	0.75	0	1
5	1	0	1
6	2	0	1
7	∞	(transverse stress only)	
8	0.5	180°	1
9	1	180°	1
10	2	180°	1
11	3	180°	1
12	1	0	2
13	1	90°	2
14	1	0	3
15	1	180°	3

TABLE 1 TEST CONDITIONS ON THIN WALL TUBES FROM McDIARMID [7]. FOR ALL TESTS σ_1 IS LONGITUDINAL AND σ_2 IS TRANSVERSE

Thin Wall Cylinders, Stresses In-Phase and Out-of-Phase at Different Frequencies

Tests[7] were conducted at λ =1, in-phase and 90° out-of-phase at frequency ratio (α) of 2, and also at λ = 1, in-phase and 180° out-of-phase at a frequency ratio of 3; as shown in Table 1 for cases 12 to 15. In all four test cases Case A longitudinal cracks occurred.

In these test cases where the biaxial principal stresses are of the same amplitude but of different frequency, it has been shown [15] that the frequency difference causes the critical shear stress and associated normal stress on the same plane to have varying amplitudes and thus there is a cumulative damage problem. It is also clear that these stresses are out-of-phase.

For each cycle of σ_{1a} we obtain a number of cycles of τ_{12} and $\sigma_{n,12}$ of different amplitude depending on the value of the frequency ratio. Values of τ_{12} and $\sigma_{n,12}$ for cases 12 to 15, taken from ref. (15) are shown in Table 3. For both shear and normal stresses, only the cycles of greatest amplitude are considered to be damaging. Table 3 shows that some allowance would have to be made for the damaging effect of the lesser shear stress amplitudes which are 35% and 50% of the greater shear stress amplitudes in cases 13 and 15 respectively.

Thin Wall Cylinders with Mean Stress and Out-of-Phase Stresses at Different Frequencies

Finally [8] tests were conducted with longitudinal, transverse and both longitudinal and transverse mean stresses, respectively for eight different (λ, ϕ, α) values, producing

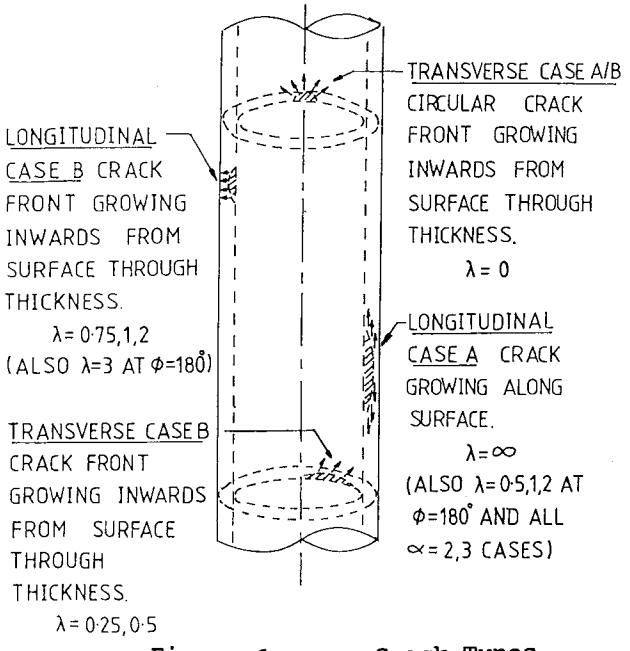

Figure 6. Crack Types.

three different Cases of crack growth as follows:-

Case A/B transverse, circular crack front: Longitudinal stress only

Case B longitudinal: Transverse stress only and (1, 0°, 1)

Case A longitudinal: (1, 180°, 1), (1, 0°, 2), (1 90°, 2), (1, 0°, 3), (1, 180°, 3).

Test conditions are shown in Table 4 and the stress conditions on the critical shear planes are described in Table 4 of ref. (8). Crack Cases for test cases 1 to 8 of ref. (8) are given in Table 5.

Case	λ	Critical Shear Plane	$\frac{\tau_a}{\sigma_{1a}}$	$\frac{\sigma_n}{\sigma_{1a}}$	Applied Stress Amplitudes at 10^6 cycles, MN/m^2 Long'l (σ_{1a})	Trans (σ_{2a})	Critical Shear Stress Amplitude at 10^6 cycles, MN/m^2	Crack Case and Direction
	$\phi = 0°$:-							
1	0	12,31	0.5	0.5	465	0	230	A/B Transverse
2	0.25	31	0.5	0.5	525	131	260	B Transverse
3	0.5	31	0.5	0.5	500	250	250	B Transverse
4	0.75	23(31)	0.38(0.5)	0.38(0.5)	465	350	230	B Long'l/Trans
5	1	23	0.5	0.5	350	350	175	B Longitudinal
6	2	23	1	1	180	365	180	B Longitudinal
7	∞	23	$0.5\sigma_{2a}$	$0.50\sigma_{2a}$	0	350	175	A Longitudinal
	$\phi = 180°$:-							
8	0.5	12	0.75	0.25	400	200	300	A Longitudinal
9	1	12	1	0	280	280	280	A Longitudinal
10	2	12	1.5	0.5	170	340	255	A Longitudinal
11	3	23	1.5	1.5	110	330	165	B Longitudinal

TABLE 2 STRESSES ON THE CRITICAL SHEAR PLANES FOR CASES 1 TO 11 FROM McDIARMID [7]

Thin Wall Cylinders with Out-of-Phase Loading Including Different Waveforms and Frequencies

Dietmann et al [16] conducted tests on thin wall steel tubular specimens under pulsating internal pressure and pulsating axial tension for the range of waveform shapes, out-of-phase angles and frequency ratios shown in Figure 7. The shear and normal stresses on the plane of maximum range of shear stress are non-proportional and out-of-phase. Test cases 1, 5 and 6 produce Case B longitudinal cracks while all other cases produce Case A longitudinal cracks.

Correlation of Thin Wall Cylinder Test Data with Failure Criterion

Test data from McDiarmid[7], covering the test conditions listed in Table 1

Test series	λ	ϕ	α
1	0	(Longitudinal stress only)	
2	∞	(Transverse stress only)	
3	1	0°	1
4	1	180°	1
5	1	0°	2
6	1	90°	2
7	1	0°	3
8	1	180°	3

Series 1.1, 2.1 etc — Zero mean stress
Series 1.2, 2.2 etc — Longitudinal mean stress
Series 1.3, 2.3 etc — Transverse mean stress
Series 1.4, 2.4 etc — Both longitudinal and transverse mean stresses

TABLE 4 TEST CONDITIONS FOR TEST SERIES 1 TO 8 FROM McDIARMID[8]

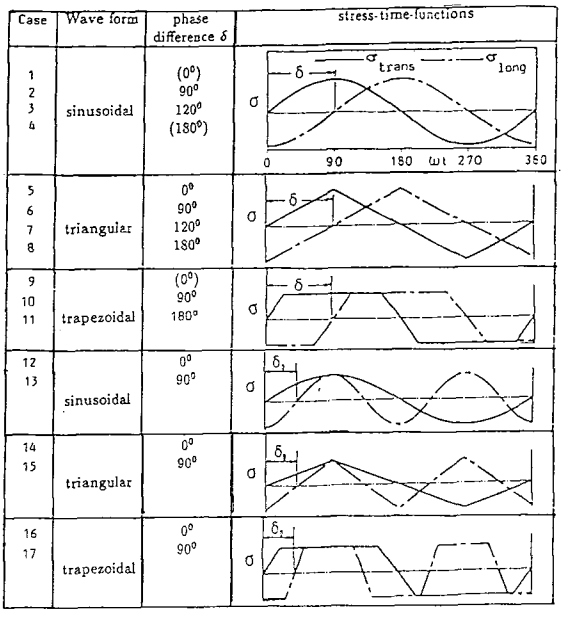

Figure 7.

Dietmann et al (16) Test Programme for Different Wave Forms.

Case	Long'l Stress σ_{1a} at 10^6 cycles MN/m^2	$\frac{\tau_a}{\sigma_{1a}}$	$\frac{\sigma_n}{\sigma_{1a}}$	Critical Shear Stress Amplitude τ_{12} at 10^6 cycles, MN/m^2
12	294	0 ± 0.88 0 ± 0.18	0 ± 0.88 0 ± 0.18	259
13	294	0 ± 0.78 0.28 ± 0.28	-0.12 ± 0.78 0.28 ± 0.28	230
14	270	0 ± 1.00 0 ± 0.26 0 ± 0.26	0 ± 0.76 0.38 ± 0.38 -0.38 ± 0.38	270
15	270	0 ± 0.76 0 ± 0.38 0 ± 0.38	0 ± 1.00 0 ± 0.26 0 ± 0.26	205
9	278	0 ± 1.0	0	278

TABLE 3 STRESSES ON THE CRITICAL SHEAR PLANES FOR CASES 12 TO 15 FROM McDIARMID [7]

Test Series	Test Case in Ref [7]	Critical Shear Plane	Crack Case
1	1	12 = 31	Transverse A/B circular into surface
2	7	23	Longitudinal B into surface
3	5	23	Longitudinal B into surface
4	9	12	Longitudinal A along surface
5	12	12	Longitudinal A along surface
6	13	12	Longitudinal A along surface
7	14	12	Longitudinal A along surface
8	15	12	Longitudinal A along surface

TABLE 5 CRITICAL SHEAR PLANES AND CRACK CASES FROM McDIARMID [8]

where the biaxial stresses can be in-phase, out-of-phase and at different frequencies is compared with the failure criterion in Figure 8 where it is seen that all data except that for Case B longitudinal cracks growing inwards from the surface (test cases 5, 6, 7 and 11) correlate reasonably well. The t_A value used in Figure 8 is that obtained from test case 9 ($\lambda = 1, \phi = 180°$), that is pure reversed shear stress for Case A longitudinal cracks growing along the surface. A t_B value for pure reversed shear stress for Case B longitudinal cracks growing inwards from the surface has to be used to correlate the test data for this type of cracking.

Test data from reference (8), that is with mean stress, is compared with the failure criterion in Figure 9 where similar correlation as that for reference (7) data is confirmed. Some of the cases 6 and 8 data from reference (8) gives poor correlation because of the cumulative damage effect occurring as described earlier.

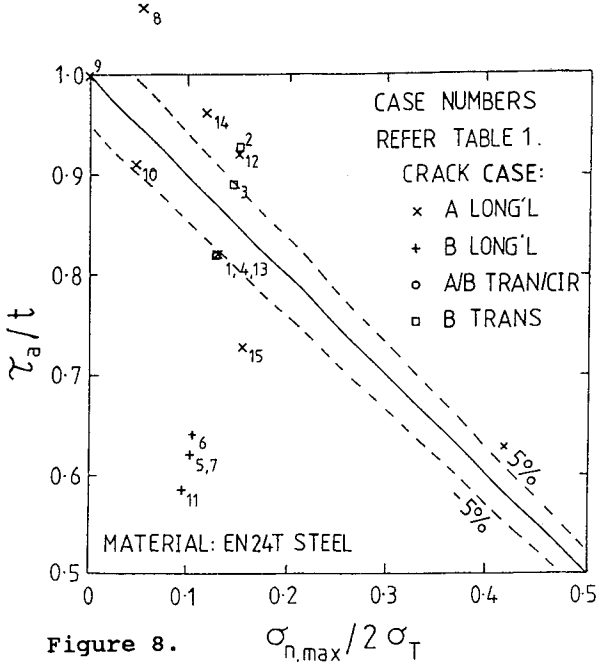

Figure 8. Correlation of McDiarmid (7) Thin Wall Cylinder Data with Failure Criterion.

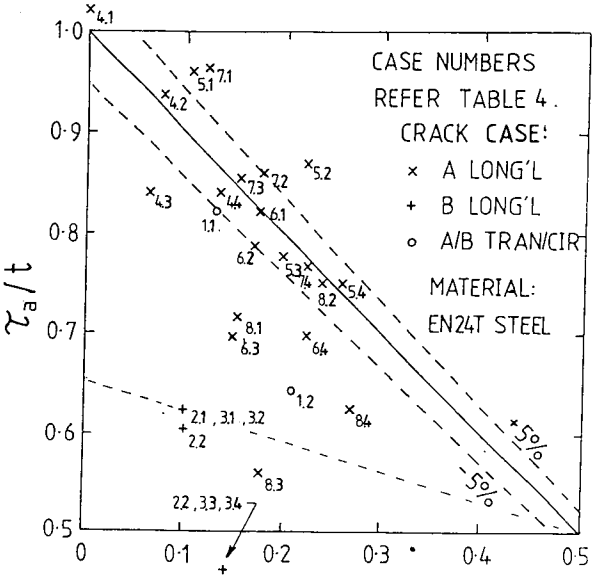

Figure 9. $\sigma_{n,max}/2\sigma_T$

Correlation of McDiarmid (8) Thin Wall Cylinder with Mean Stress Data with Failure Criterion.

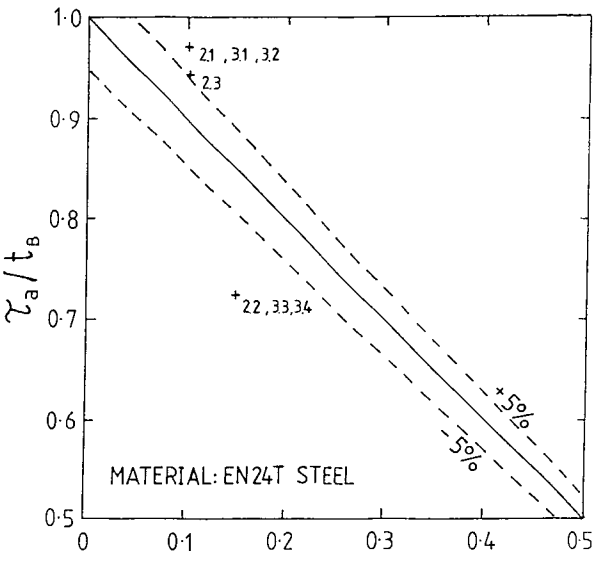

Figure 10. $\sigma_{n,max}/2\sigma_T$

Correlation of McDiarmid (8) Thin Wall Cylinder with Mean Stress Data with Failure Criterion, for Case B Crack Growth.

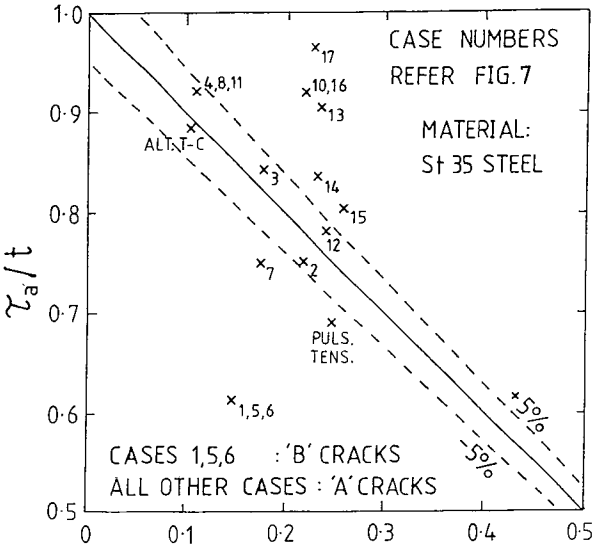

Figure 11. $\sigma_{n,max}/2\sigma_T$

Correlation of Dietmann et al (16) Thin Wall Cylinder Data with Failure Criterion.

A t_B value for correlating Case B longitudinal crack data can be found as indicated in Figure 9 by extrapolating a straight line from $\sigma_{n,max}/2\sigma_T$ equal to 0.5 through, say, the point for test case 2.1 (8) to give $\tau/t_B = 0{\cdot}65$ as indicated. The Case B longitudinal crack data is then compared with the failure criterion as shown in Figure 10. It appears that the mean shear stress occurring on the critical shear plane may be more significant for the Case B longitudinal cracks than for the Case A longitudinal cracks.

Test data from the Dietmann(16) programme for different waveforms, as shown in Figure 7 is compared with the failure criterion in Figure 11. Test cases 1, 5 and 6 produce Case B cracks growing inwards from the surface while all other test cases produce Case A cracks growing along the surface. All Case A crack data falls within ±5% of the failure criterion except for cases 10 and 12 to 17 where τ and $\sigma_{n,max}$ are out-of-phase, $\sigma_{n,max}$ being zero when τ is a maximum, thus the failure criterion errs on the conservative side. This effect is illustrated in reference (6).

Thick Wall Cylinders

Morrison et al(17) conducted an extensive series of investigations of the fatigue strength of thick wall cylinders of several materials (see Table 6) over a range of wall thickness to diameter ratio, subjected to pulsating internal oil pressure. The results of these tests showed that the fatigue strength of the thick cylinders, in terms of maximum shear stress amplitude, was about half that found from solid torsion fatigue tests. They suggested that the pulsating high pressure oil in intimate contact with the cylinder bore may cause a decrease in fatigue strength and showed, in a small number of tests, in which the cylinders bores were protected by a neoprene coating that the fatigue strength was increased.

In the light of the discussion here and in reference (7) on the different types of crack growth systems which can occur in multiaxial fatigue it is not surprising that the thick cylinder test

MATERIAL	TENSILE STRENGTH MN/m^2	FATIGUE STRENGTH SOLID SPECIMENS MN/m^2		RANGE OF PULSATING FATIGUE STRENGTH (10^7 CYCLES) OF THICK CYLINDERS (SHEAR) MN/m^2				
		TORSION	TRANSVERSE BENDING	K=1.2	1.4	1.6	1.8	2.0	3.0
VIBRAC Ni Cr Mo STEEL	867.7	301.1	432.3	285.6	277.9	285.6	277.9	270.2	293.4
VIBRAC AUTOFRETTAGED	867.7		432.3			316.5		362.8	
VIBRAC	1025.2	364.4	506.4		362.8		362.8		
HYKRO Cr Mo STEEL	830.7	287.2	406.1		285.6			293.4	
HYKRO NITRIDED BORE						447.8			
0.15% C STEEL	393.7	135.9	189.9		123.5			131.2	
18/8% Cr Ni Ti STEEL	591.4	183.7 to 219.2	381.4		162.1			254.8	
Al-Cu ALLOY	503.3	95.7	185.3					139.0	
TITANIUM, COMM PURE	413.8	157.5	277.9		169.8			200.7	

TABLE 6 THE STRENGTH OF THICK CYLINDERS SUBJECTED TO INTERNAL PRESSURE, MORRISON ET AL [17] REPRODUCED FROM FORREST [18]

data in terms of maximum shear stress amplitude did not agree with torsion fatigue test data. In the torsion tests Case A cracks growing along the surface occur whereas in the thick cylinder tests Case B cracks growing inwards from the surface occur.

A value of t_B can be obtained for the thick cylinder materials tested from the values of transverse rotating bending fatigue strengths given in reference [17], which produce Case B cracks growing inwards from the surface along the length of the material as they do in the thick cylinder case. This is done using the τ versus $\sigma_{n.max}$ diagram, projecting a straight line from $2\sigma_T$ on the $\sigma_{n.max}$ axis through the $(\tau, \sigma_{n.max})$ point representing the transverse rotating bending fatigue strength to obtain t_B on the τ axis. Then using hoop stresses augmented by the internal pressure value to allow for the oil pressure acting in the crack effect, τ/t_B versus $\sigma_{n.max}/2\sigma_T$ data are obtained which showed the failure criterion to be optimistic. However, t_B values used were derived from transverse rotating bending fatigue tests in air. It is noted from reference [17] that push-pull fatigue tests in an oil bath at 300 MN/m^2 unprotected gave a fatigue limit, 0.85 that in the protected case. Applying this 'correction' factor to t_B values the failure criterion gives the correlation with test data shown in Figure 12. All test data lies within about ±10% of the failure criterion.

It is noted that fatigue strength increases with increase in k (equal to ratio of outer to inner cylinder diameter) for all the materials tested. This could be due to the oil pressure effect within the crack being fully effective for a greater proportion of the life for the thinner specimens.

Discussion

The criterion of multiaxial fatigue failure

$$\tau_a/t_{A,B} + \sigma_{n.max}/2\sigma_T = 1$$

has been shown to give good correlation with extensive high cycle multiaxial fatigue data from the literature under a wide variety of multiaxial loading conditions.

For Case A cracks growing along the surface, as in combined bending and twisting, t_A = t, the torsion fatigue strength. When Case A cracks occur in cylinders t_A = t can be used.

When Case B cracks growing inwards from the surface occur, t_B can be found using the failure criterion line to extrapolate through a Case B crack data point, if known, to the $\sigma_{n.max} = 0$ case. In the case of thick cylinders the transverse bending fatigue strength can be used, as this loading produces Case B cracks growing in the same longitudinal plane as they do in pressurised thick cylinders.

The uniaxial longitudinal fatigue case (λ=0)is special in that theoretically it

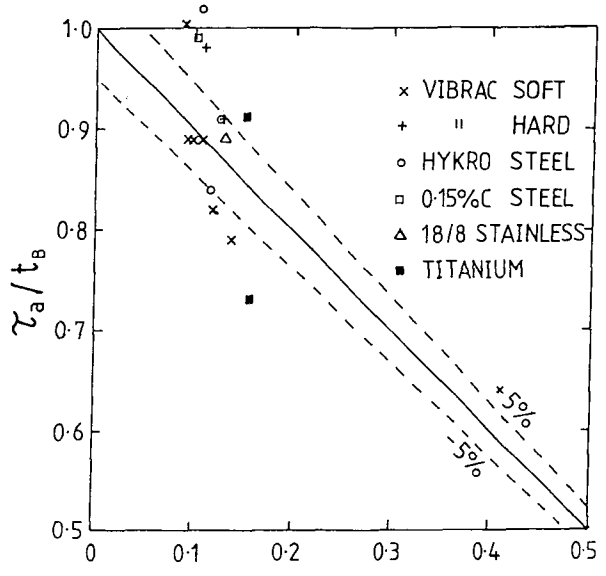

Figure 12.

Correlation of Morrison et al (17) Thick Cylinder Data with Failure Criterion.

produces equal amounts of Case A and Case B cracking. As λ becomes positive Case B cracking predominates, whereas when λ becomes negative Case A cracking will predominate. This interim region of Case A/B cracking will also be affected by material anisotropy relative to the orientation of the principal stresses. These are effects which require further study. A 15% to 20% decrease in fatigue strength in the transverse direction is commonly reported [18] although the effect can be greater in some materials.

Multiaxial stresses which are out-of-phase, at different frequencies or of a non-sinusoidal wave form have been shown to cause non-proportional stress effects which can create complex cumulative damage problems. The effects of cumulative damage in multiaxial fatigue has as yet seen very limited study.

In the general case of structural fatigue analysis the type of cracking occurring, Case A or B, can be determined from a study of surface strain records. Figure 13 indicates one means of determining the allowable principal surface strains, as described in reference (19).

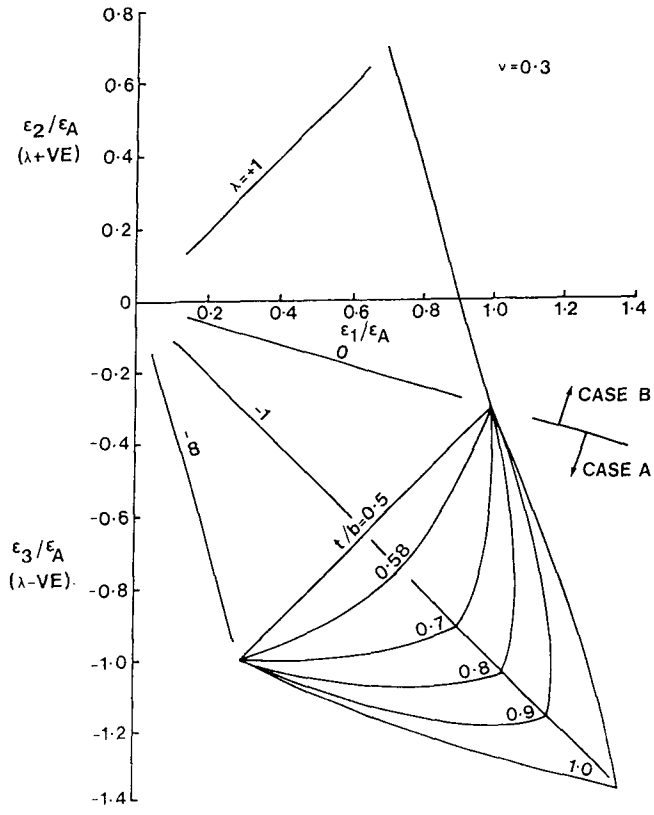

Figure 13.

Allowable Principal Surface Strains From McDiarmid (19).

Conclusion

A simple general criterion of failure for high cycle multiaxial fatigue

$$\tau_a / t_{A,B} + \sigma_{n.max.} / 2\sigma_T = 1$$

is presented and found to give good correlation with a wide variety of multiaxial fatigue test data.

The criterion is based on a critical plane approach where fatigue strength is a function of the shear stress amplitude and the maximum normal stress on the critical plane of maximum shear stress amplitude, taking account of whether Case A cracks, growing along the surface, or Case B cracks growing inwards from the surface occur. The criterion is applicable in the region $0{\cdot}5t \leq \tau_a \leq t$, $0 \leq \sigma_{n.max.} \leq \sigma_T$.

References

1 BROWN, M.W. and MILLER, K.J. (1973). A theory for fatigue failure under multiaxial stress strain conditions. Proc. Inst. Mech. Engrs. 187(65-73), 745-755

2 GARUD, Y.S. (1981). Multiaxial fatigue: A Survey of the state of the art. J. Test. Eval. 9, 165-178.

3 JORDAN, E.H. (1982). Fatigue-Multiaxial aspects. J. Press. Vess. Piping: a decade of progress. Am. Soc Mech. Engrs. 507-520

4 PAPADOPOULOS, Y. (1987). On the multiaxial fatigue of metals. (In French). L'ecole nationale des ponts et chaussées. Ph.D. Thesis

5 FATEMI, A. and SOCIE, D.F. (1988). A critical plane approach to multiaxial fatigue damage including out-of-phase loading. Fatigue Fract. Engng. Mater. Struct., 11, 3, 149-165

6 McDIARMID, D.L. A general criterion for high cycle multiaxial fatigue failure. Fatigue Fract. Engng. Mater. Struct. To be published.

7 McDIARMID, D.L. (1989) Crack systems in multiaxial fatigue. Advances in Fracture Research. Proc. Seventh Int. Conf. on Fracture, Ed. Salama, K et al, Pergamon, 1265-1277

8 McDIARMID, D.L. (1989) Mean stress effects in biaxial fatigue where the stresses are out-of-phase and at different frequencies. Proc. Third Int. Conf. on Biaxial/Multiaxial Fatigue, Stuttgart, West Germany. To be published in EGF series by MEP Publications Ltd, London.

9 MILLER, K.J. and BROWN, M.W. (1985). Multiaxial fatigue: a brief review. Advances in Fracture Research. Ed. Rao, P.R. et al., Pergamon, London 31-56

10 GOUGH, H.J., POLLARD, H.V. and CLENSHAW, W.J. (1951) Some experiments on the resistance of metals to fatigue under combined stress. Aero Research Council, R and M 2522, H.M.S.O., London

11 McDIARMID, D.L. (1985). The effects of mean stress and stress concentration on fatigue under combined bending and twisting. Fatigue Fract. Engng. Mater. Struct., 8, 1, 1-12

12 NISHIHARA, T. and KAWAMOTO, M. (1945). The strength of metals under combined bending and twisting with phase differences. Memoirs, College of Engineering, Kyoto Imperial University, Vol. XI, 85-112

13 LITTLE, R.E. (1969). A note on the shear stress criterion of failure under combined stress. Aeronaut, Q. 20, 57-60

14 McDIARMID, D.L. (1987). Fatigue under out-of-phase bending and torsion. Fatigue Fract. Engng. Mater. Struct., 9, 6, 457-475

15 McDIARMID, D.L. (1985). Fatigue under out-of-phase biaxial stresses of different frequencies. A.S.T.M. S.T.P. 853, 606-621

16 DIETMANN, H., BHONGHIBHAT, T. and SCHMID, A. (1989). Multiaxial fatigue behaviour of steels under in-phase and out-of-phase loading including different wave forms and frequencies. Proc. Third Int. Conf. on Biaxial/Multiaxial Fatigue, Stuttgart, West Germany

17 MORRISON, J.L.M., CROSSLAND, B. and PARRY, J.S.C. (1960). Strength of thick cylinders subjected to repeated internal pressure. Proc. I. Mech. E., Vol. 174(2), 95-117

18 FORREST, P.G. (1962). Fatigue of metals. Pergamon Press, London

19 McDIARMID, D.L. (1985). Designing for high cycle biaxial fatigue using surface strain records. Multiaxial Fatigue, ASTM STP 853. Ed., K.J. Miller and M.W. Brown. American Society for Testing and Materials, Philadelphia, 431-439